Detection of Coexisting Fluid Phospholipid Phases by Equilibrium Ca^{2+} Binding: Peptide-Poor L_α and Peptide-Rich H_{II} Phase Coexistence in Gramicidin A′/Phospholipid Dispersions†

Andrew R. G. Dibble‡ and Gerald W. Feigenson*

Section of Biochemistry, Molecular and Cell Biology, Cornell University, Ithaca, New York 14853

Received April 19, 1994; Revised Manuscript Received August 23, 1994®

ABSTRACT: The isothermal phase behavior of three gramicidin A′/phospholipid mixtures was investigated by an equilibrium Ca^{2+}-binding technique. The phospholipid component was 1,2-dioleoyl-*sn*-glycero-3-phosphoserine (DOPS), 1-palmitoyl-2-oleoyl-*sn*-glycero-3-phosphoserine (POPS), or POPS/1-palmitoyl-2-oleoyl-*sn*-glycero-3-phosphocholine (POPC) at a constant mole ratio of 1/4. The bulk aqueous free Ca^{2+} concentration, $[Ca^{2+}]^*_f$, in equilibrium with one or two gramicidin A′/phospholipid fluid phases and a small amount of the Ca(phosphatidylserine)$_2$ gel phase, was measured as a function of composition at 20 °C by use of chromophoric high-affinity Ca^{2+} chelators. The coexistence of two gramicidin A′/phospholipid fluid phases was detected by an invariance in $[Ca^{2+}]^*_f$ over the range of compositions throughout which the two phases coexist. The compositions of the two coexisting phases are determined by the compositions at which the invariance in $[Ca^{2+}]^*_f$ begins and ends. With each of the gramicidin A′/phospholipid mixtures, we estimate that the composition of the gramicidin-poor phase is 0.03–0.04 mole fraction gramicidin A′ and the composition of the gramicidin-rich phase is 0.13–0.14 mole fraction gramicidin A′. Characterization of these phases by low-angle X-ray diffraction revealed that, in each case, the gramicidin-poor phase is an L_α phase and the gramicidin-rich phase is an H_{II} phase. The isothermal phase behavior of gramicidin A′/POPC mixtures at ~23 °C, as determined by low-angle X-ray diffraction, was found to be similar to that of the other gramicidin A′/phospholipid mixtures. ^{31}P nuclear magnetic resonance spectroscopy failed to detect the gramicidin-rich H_{II} phase in all cases except when the phospholipid component was DOPS. The general applicability of the equilibrium Ca^{2+}-binding technique to the detection of phospholipid phase separations, including L_α^1/L_α^2 phase separations, is discussed.

Most biological membranes are composed of complex mixtures of lipids and proteins. Evidence for significant lateral heterogeneity of lipid and protein components in many types of cell and model membranes has been provided by a wide variety of experimental techniques [for reviews, see Edidin (1992) and Tocanne (1992)]. Some of these lateral heterogeneities in cell membranes appear to be caused by interactions with cytoskeletal elements or by the addition or depletion of components in specialized areas by membrane fusion or budding. In addition to these kinds of external mechanisms, thermodynamically nonideal (i.e., nonrandom) mixing of the membrane components might be important. Nonideal mixing could give rise to a clustering of a subset of the components in a single lipid phase. In cases of extreme positive deviations from ideal mixing, an additional macroscopic lipid phase could form.

It is clear that a direct way to probe for the existence of either microscopic clusters or macroscopic phase separations in membranes is to ascertain the degree to which the components deviate from ideal mixing behavior [see discussion in Wolf (1992)]. A proper way to characterize this mixing behavior is to determine the thermodynamic activities of the membrane components as a function of composition. Our laboratory has developed a method by which the thermodynamic activity of PS,[1] a_{PS}, in fluid lipid bilayers can be determined as a function of composition in model membranes (Huang et al., 1993). The evaluation of a_{PS} in the fluid lipid phase relies on measurements of aqueous free Ca^{2+} concentration, $[Ca^{2+}]^*_f$, in equilibrium with the fluid phase and a small amount of a Ca^{2+}-induced PS gel phase. This gel phase has the stoichiometry Ca(PS)$_2$ (Feigenson, 1986) and has been characterized by differential scanning calorimetry and X-ray diffraction (Portis et al., 1979; Hauser & Shipley, 1984) as well as by electron paramagnetic resonance and fluorescence techniques (Florine & Feigenson, 1987). The Ca(PS)$_2$ phase is essentially a pure phase, containing almost no PC (Florine & Feigenson, 1987) or gramicidin A′ (Dibble et al., 1993). For the purpose of measuring thermodynamic properties of PC/PS or gramicidin A′/PS model membranes, the essential features of the system are described by the heterogeneous chemical equilibrium (Feigenson, 1989):

† This work was supported by a grant from the National Institutes of Health, U.S. Public Health Service (HL-18255). A.D. was supported in part by National Institutes of Health Research Service Awards 5T32GM07273 and 5T32GM08384.

* Author to whom correspondence should be addressed.

‡ Present address: Department of Pharmacology, University of Virginia Health Sciences Center, Charlottesville, VA 22908.

® Abstract published in *Advance ACS Abstracts,* October 1, 1994.

[1] Abbreviations: DPPC, 1,2-dipalmitoyl-*sn*-glycero-3-phosphocholine; DOPC, 1,2-dioleoyl-*sn*-glycero-3-phosphocholine; DOPS, 1,2-dioleoyl-*sn*-glycero-3-phosphoserine; POPC, 1-palmitoyl-2-oleoyl-*sn*-glycero-3-phosphocholine; POPS, 1-palmitoyl-2-oleoyl-*sn*-glycero-3-phosphoserine; PC, phosphatidylcholine; PS, phosphatidylserine; Ca(PS)$_2$, Ca^{2+}-induced PS gel phase; $[Ca^{2+}]_f$, free Ca^{2+} concentration in the bulk aqueous phase; $[Ca^{2+}]^*_f$, $[Ca^{2+}]_f$ at equilibrium; $[Ca^{2+}]^*_{f,\chi_{gr}=0}$, $[Ca^{2+}]^*_f$ at 0 mole fraction gramicidin A′; $[Ca^{2+}]^*_{f,\chi_{POPC}=0}$, $[Ca^{2+}]^*_f$ at 0 mole fraction POPC; BrBAPTA, 1,2-bis(*o*-amino-5-bromophenoxy)ethane-*N,N,N′,N′*-tetraacetic acid; MeBAPTA, 1,2-bis(*o*-amino-5-methylphenoxy)ethane-*N,N,N′,N′*-tetraacetic acid; K_D, dissociation constant; Pipes, piperazine-*N,N′*-bis(2-ethanesulfonic acid); NMR, nuclear magnetic resonance; a_{PS}, thermodynamic activity of PS; χ_{gr}, mole fraction of gramicidin A′; χ_{POPC}, mole fraction of POPC.

0006-2960/94/0433-12945$04.50/0

$$Ca^{2+}_{(aqueous)} + 2PS^{-}_{(hydrated)} \rightleftharpoons Ca(PS)_2 + nH_2O \quad (1)$$

Establishment of this chemical equilibrium and the measurement of $[Ca^{2+}]^*_f$ as a function of composition lead to a determination of a_{PS} as a function of composition. Using this equilibrium Ca^{2+}-binding approach, we have previously shown that the components of several PC/PS mixtures exhibit significant positive deviations from ideal mixing (i.e., PC–PC and PS–PS interactions favored over PC–PS interactions) within the L_α phase at low aqueous free Ca^{2+} concentrations (i.e., <10 μM), despite the electrostatic repulsion between PS headgroups (Huang et al., 1993).

We are also interested in the mixing behavior of phospholipids and membrane proteins in fluid bilayers. Here we address this issue by using the equilibrium Ca^{2+}-binding technique to analyze gramicidin A′/DOPS, gramicidin A′/POPS, and gramicidin A′/(POPS/POPC; 1/4, mol/mol) mixtures. Gramicidin A′ is a linear pentadecapeptide, two monomers of which span the bilayer in the $\beta^{6.3}$-helical conformation (Urry, 1971; Urry et al., 1971). This peptide is a convenient model for the membrane-spanning domain of transmembrane proteins. Our results indicate extreme positive deviations from ideal mixing, with fluid–fluid phase separation occurring over a wide range of compositions with all three systems. This macroscopic phase separation involves the coexistence of a gramicidin-poor (0.03–0.04 mole fraction gramicidin A′) L_α phase and a gramicidin-rich (0.13–0.14 mole fraction gramicidin A′) H_{II} phase.

Coexisting L_α and H_{II} phospholipid phases have been observed before in a variety of systems (Seddon, 1990), including gramicidin A′/phospholipid dispersions (Killian, 1992). The most common experimental techniques used to discern the coexistence of L_α and H_{II} phases are low-angle X-ray diffraction (Luzzati, 1980), ^{31}P NMR spectroscopy (Cullis & de Kruijff, 1979), and freeze-fracture electron microscopy (Verkleij, 1984). This paper introduces our equilibrium Ca^{2+}-binding technique as a novel way to detect coexisting fluid phospholipid phases. An advantage of the equilibrium Ca^{2+}-binding method is that it is a thermodynamic approach which detects phase separations and defines phase boundaries by application of the Gibbs phase rule. Thus, it is a generally applicable method which can be used to probe for a variety of types of phospholipid phase separations, including L_α^1/L_α^2 phase separations, which may not be easily detectable by other techniques.

EXPERIMENTAL PROCEDURES

Materials

Phospholipids were from Avanti Polar Lipids, Inc. (Birmingham, AL) and were judged to be >99% pure by thin-layer chromatography of 0.1 mg of each lipid on Adsorbosil-Plus 1 P* plates (Alltech Associates, Inc., Deerfield, IL), using chloroform/methanol/concentrated ammonium hydroxide (65/25/5, v/v/v). The natural mixture of gramicidins A, B, and C from *Bacillus brevis* was purchased from Serva Biochemicals (Westbury, NY). The mixture of gramicidins A, B, and C is referred to as gramicidin A′. The chromophoric high-affinity Ca^{2+} chelators BrBAPTA and MeBAPTA were obtained from Molecular Probes, Inc. (Eugene, OR). Chelex-100 ion-exchange resin was analytical grade from Bio-Rad Laboratories (Rockville Centre, NY). Pipes buffer was BioChemika MicroSelect grade from Fluka Chemical Corp. (Ronkonkoma, NY). Water was purified with a Milli-Q system (Millipore Corp., Bedford, MA). Chloroform and methanol (HPLC grade) were from Mallinckrodt, Inc. (Paris, KY). All other chemicals were reagent grade.

Methods

Preparation of Solutions. Ca^{2+}-free buffer (5 mM Pipes, 100 mM KCl, pH 7.0) was prepared by passing the buffer through a Chelex-100 ion-exchange column. The Ca^{2+} concentration in the eluant was subnanomolar. The BrBAPTA and MeBAPTA standard solutions in Ca^{2+}-free buffer were prepared essentially as described (Feigenson, 1986). The primary standard Ca^{2+} solution in buffer was prepared from an analytical concentrate of $CaCl_2$ (J. T. Baker, Inc., Phillipsburg, NJ). The phospholipid concentration of stock solutions of DOPS, POPS, or POPC in chloroform was periodically determined by phosphorus analysis (Kingsley & Feigenson, 1979). The concentration of gramicidin A′ in methanolic solution was periodically determined spectrophotometrically, using ϵ_{280} = 20.7 $cm^{-1}\cdot mM^{-1}$ (Killian et al., 1988). All stock solutions were stored under an argon atmosphere, at -20 °C.

The Ca^{2+}-Binding Assay. The measurement of the equilibrium free Ca^{2+} concentration, i.e., $[Ca^{2+}]^*_f$, in the bulk aqueous phase of PS-containing samples was done essentially as previously described (Huang et al., 1993). In brief, dispersions of gramicidin A′ together with DOPS, POPS, or POPS/POPC (1/4, mol/mol) were prepared from mixtures which had been freeze-dried from benzene/methanol (19/1, v/v). After at least 2 h of hydration time with Ca^{2+}-free buffer, the samples were exposed to Ca^{2+} by the addition of $CaCl_2$ and a chromophoric Ca^{2+} chelator. After this addition, the samples had a total chelator concentration of 85–140 μM, a total Ca^{2+} concentration of 85–200 μM, and a bulk aqueous free Ca^{2+} concentration, $[Ca^{2+}]_f$, of 0.1–100 μM. $[Ca^{2+}]_f$ then decreased with time due to Ca^{2+}-binding to PS headgroups between lamellae to form the $Ca(PS)_2$ phase. Ca^{2+}-binding was allowed to continue until 5–15% of the PS had been recruited to the $Ca(PS)_2$ phase (usually 1–2 weeks). The equilibrium value of $[Ca^{2+}]_f$, $[Ca^{2+}]^*_f$, was determined by dissolving 10–30% of the $Ca(PS)_2$ phase by means of the addition of Ca^{2+}-free chelator. Equilibrium was judged to have been reached when $[Ca^{2+}]_f$ no longer varied with additional $Ca(PS)_2$-dissolving steps or longer incubation times. The final amount of PS in the $Ca(PS)_2$ phase was only 5–10% of the total PS in the sample.

During the course of the assay, $[Ca^{2+}]_f$ was determined spectrophotometrically, following Tsien (1980) and Feigenson (1986). Periodically, aliquots (150–200 μL) of the aqueous phase above the settled lipid (0.5–1.0 μmol of PS in an initial volume of 1.0 mL) were removed for measurement of $[Ca^{2+}]_f$. In order to reduce light scattering caused by traces of suspended lipid, the aliquots were centrifuged for at least 1 h at 22000g in an SW-27 swinging-bucket rotor at 20 °C, using 400-μL polypropylene centrifuge tubes supported in 2 M sorbitol. The supernatants were analyzed for $[Ca^{2+}]_f$ as follows. Absorbance was measured, using a Hewlett Packard 8452A spectrophotometer, at the isosbestic point (248.6 nm for BrBAPTA, 240.0 nm for MeBAPTA) and the peak of the difference spectrum (i.e., Ca^{2+}-free chelator minus Ca^{2+}-saturated chelator; 262 nm for BrBAPTA, 256 nm for MeBAPTA). These measurements were used to calculate $[Ca^{2+}]_f$ from

$$[Ca^{2+}]_f = K_d[Ca\cdot Chel]/[Chel] = K_d(A'_0 - A')/(A' - A'_1) \quad (2)$$

where Chel is Ca^{2+}-free chelator, Ca·Chel is Ca^{2+}-saturated

chelator, and A, A_0, and A_1 are the absorbances of the sample of interest, Ca^{2+}-free chelator, and Ca^{2+}-saturated chelator, respectively, at the peak of the difference spectrum. The primes indicate division by the absorbance at the isosbestic point. The A'_0 values used for BrBAPTA and MeBAPTA were 1.52 and 1.33, respectively. The A'_1 values used were 0.25 and 0.15, respectively. The K_D values for BrBAPTA and MeBAPTA were determined essentially as described (Feigenson, 1986); for this buffer system they were measured to be 1.4 μM and 63 nM, respectively.

In order to ensure that the Ca^{2+}-chelators did not degrade significantly over the long time course of these experiments, $[Ca^{2+}]_f$ was calculated at multiple wavelengths for all samples. Changes in the absorbance spectra of the Ca^{2+} chelators upon prolonged exposure to light and/or oxygen cause the calculated values of $[Ca^{2+}]_f$ to vary significantly with wavelength. This proved to be a reliable and sensitive way to monitor the stability of the Ca^{2+} chelators. We found BrBAPTA and MeBAPTA to be stable for weeks, under our experimental conditions.

Alternative Protocols for Determining $[Ca^{2+}]^*_f$. Most determinations of $[Ca^{2+}]^*_f$ were as described above; this procedure is hereafter referred to as protocol I. To determine whether the results obtained by use of protocol I were equilibrium properties of the system, independent of the details of the procedure, several gramicidin A'/POPS samples were treated differently, as follows.

Protocol II: as I, except $[Ca^{2+}]_f$ was never reduced to a value below $[Ca^{2+}]^*_f$ by the addition of Ca^{2+}-free chelator. This procedure was designed to approach $[Ca^{2+}]^*_f$ by a long period of Ca^{2+} binding alone.

Protocol III: as I, except initial $[Ca^{2+}]_f$ was relatively high, and $[Ca^{2+}]_f$ was reduced to a value below $[Ca^{2+}]^*_f$ by the addition of Ca^{2+}-free chelator less than 1 day after Ca^{2+}-binding began. This procedure was designed to approach $[Ca^{2+}]^*_f$ rapidly, with the samples being in the $Ca(PS)_2$-dissolving mode during most of the incubation period.

Protocol IV: as I, except the lipid was supported on 5-μm pore size Millipore cellulose ester filters (Millipore Corp., Bedford, MA), essentially as described (Feigenson, 1989). This procedure was designed to make the inner bilayers of multilamellar vesicles more accessible to Ca^{2+}.

Low-Angle X-ray Diffraction. Gramicidin A'/phospholipid dispersions were prepared from mixtures which had been freeze-dried from benzene/methanol (19/1, v/v). The samples contained 3–5 μmol of phospholipid and were hydrated with 0.5–1.5 mL of 5–20 mM Pipes, 100 mM KCl, pH 7.0. The buffer contained 0.1 mM EDTA if the sample contained PS. Thus, these PS-containing samples were not identical to those examined by means of the Ca^{2+}-binding assay because we did not want to form any $Ca(PS)_2$ phase, with the attendant numerous Bragg reflections in both the low- and wide-angle regions of the diffraction pattern. After a minimum of 1 day of hydration time, each sample was transferred to a 1-mm diameter glass capillary (Charles Supper Co., Natick, MA). Lipid was concentrated by centrifugation of the capillaries in a clinical centrifuge at $\sim$2000g for up to 10 min at ambient temperature. X-ray diffraction measurements at $\sim$23 °C were made using wiggler-enhanced monochromatic X-rays at the Cornell High Energy Synchrotron Source (CHESS). X-ray diffraction patterns were recorded on X-ray sensitive film (Eastman Kodak Co., Rochester, NY).

^{31}P NMR Spectroscopy. Gramicidin A'/phospholipid dispersions were prepared as in the preceding section, except the samples contained 12.5 μmol of phospholipid and were hydrated with 0.5 mL of 20 mM Pipes, 100 mM KCl, and 20% (v/v) D_2O, pH 7.0. In order to avoid significant formation of small vesicles, the samples were not vortexed. After a minimum of 1 day of hydration time, each sample was transferred to a 5-mm diameter NMR tube. Proton noise-decoupled free induction decays were collected at 20 °C using a Varian VXRS-400 spectrometer operating at 161.9 MHz.

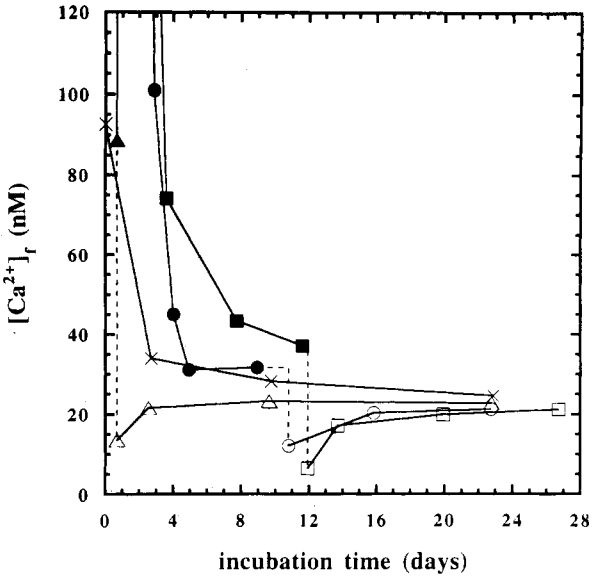

FIGURE 1: Measured values of free Ca^{2+} concentration ($[Ca^{2+}]_f$) in the bulk aqueous phase, as a function of incubation time, for typical samples of gramicidin A'/POPS multilamellar vesicles with χ_{gr} = 0.03 at 20 °C. Each sample had 1 μmol of POPS, and the Ca^{2+} chelator used was MeBAPTA. The samples were prepared by protocol I (●, ○), protocol II (×), protocol III (▲, △), and protocol IV (■, □). Initial $[Ca^{2+}]_f$ was 57 μM (protocol I), 52 μM (protocol III), and 0.9 μM (protocol IV). For Protocols I, III, and IV, solid symbols show the time course of Ca^{2+} binding between PS lamellae to form a small amount of the $Ca(PS)_2$ phase; broken lines indicate the delivery of additional Ca^{2+}-free MeBAPTA to the samples, causing $[Ca^{2+}]_f$ to drop to subequilibrium values; and open symbols show the time course of Ca^{2+} release due to the dissolving of a portion of the $Ca(PS)_2$ phase.

RESULTS

Equilibration of $[Ca^{2+}]_f$ *with Gramicidin A'/POPS Dispersions.* Most determinations of $[Ca^{2+}]^*_f$ were by use of protocol I. While the approach to equilibrium was somewhat slower at high χ_{gr}, all samples were judged to have reached an invariant value of $[Ca^{2+}]_f$ within 4 weeks. In order to confirm that the samples analyzed by protocol I had reached an equilibrium state within this period of time, the equilibration of gramicidin A'/POPS dispersions by alternate protocols was studied extensively. In general, at a given χ_{gr}, the value of $[Ca^{2+}]^*_f$ obtained was essentially independent of the protocol used (Figure 1). Indeed, the shape of the $[Ca^{2+}]^*_f$ vs χ_{gr} curve was very similar with all four protocols (data not shown). This suggests that the invariance of $[Ca^{2+}]^*_f$ observed over a wide range of compositions (see below) is an equilibrium property of the system. An exception to the independence of apparent $[Ca^{2+}]^*_f$ from the details of the $[Ca^{2+}]_f$ equilibration protocols was found with gramicidin A'/POPS dispersions when $0 < \chi_{gr} < 0.03$. With these samples, unless initial $[Ca^{2+}]_f$ was very low (i.e., $\sim$0.1 μM), protocols I, II, and III frequently led to elevated $[Ca^{2+}]^*_f$ values. These $[Ca^{2+}]^*_f$ values were not internally consistent with those at $\chi_{gr} = 0$ and $\chi_{gr} \geq 0.03$ and so were suspected to be artifacts caused by tightly sealed multilamellar vesicles. Indeed, when gramicidin A'/POPS samples were prepared by protocol IV, a procedure designed to make the inner bilayers of multilamellar vesicles more

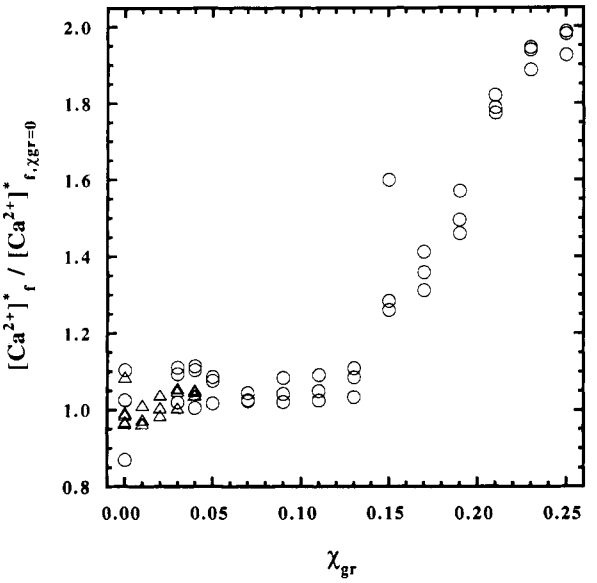

FIGURE 2: Normalized equilibrium free Ca^{2+} concentration in the bulk aqueous phase ($[Ca^{2+}]^*_f/[Ca^{2+}]^*_{f,\chi gr=0}$; denominator is 18 nM) as a function of χ_{gr} for gramicidin A′/POPS dispersions at 20 °C. Each sample had 1 μmol of POPS, and the Ca^{2+} chelator used was MeBAPTA. Triplicate samples were prepared by protocol I with an initial $[Ca^{2+}]_f$ of 0.10 μM (△) or 36–57 μM (○).

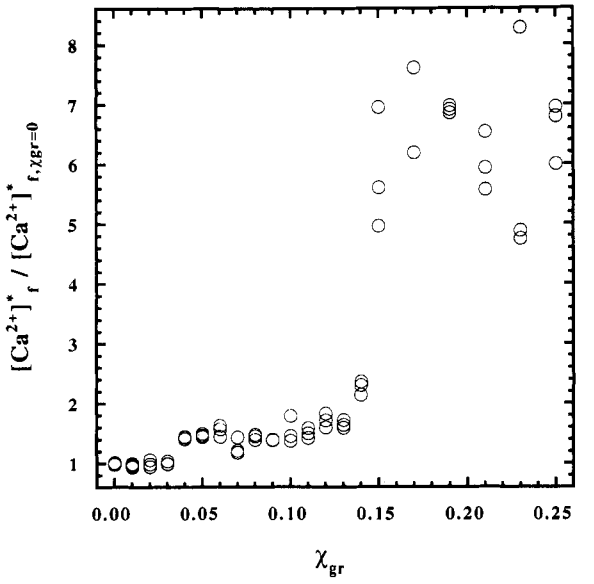

FIGURE 3: Normalized equilibrium free Ca^{2+} concentration in the bulk aqueous phase ($[Ca^{2+}]^*_f/[Ca^{2+}]^*_{f,\chi gr=0}$; denominator is 1.27 μM) as a function of χ_{gr} for gramicidin A′/(POPS/POPC; 1/4, mol/mol) dispersions at 20 °C. Each sample had 1 μmol of POPS, and the Ca^{2+} chelator used was BrBAPTA. Triplicate samples were prepared by protocol I, with an initial $[Ca^{2+}]_f$ of 43–100 μM. One datum point at χ_{gr} = 0.17 is off-scale ($[Ca^{2+}]^*_f/[Ca^{2+}]^*_{f,\chi gr=0}$ = 11.3).

accessible to Ca^{2+}, the $[Ca^{2+}]^*_f$ values at $0 < \chi_{gr} < 0.03$ were internally consistent with those at $\chi_{gr} = 0$ and $\chi_{gr} \geq 0.03$, even when initial $[Ca^{2+}]_f$ was as high as 3.5 μM.

Dependence of $[Ca^{2+}]^*_f$ on χ_{gr} in Gramicidin A′/Phospholipid Dispersions. Measurements of $[Ca^{2+}]^*_f$ as a function of composition in gramicidin A′/phospholipid dispersions gave rise to the curves shown in Figures 2–4. $[Ca^{2+}]^*_f$ was found to be essentially invariant over a wide range of compositions for each of the gramicidin A′/phospholipid mixtures analyzed. We attribute this behavior to the coexistence of two phospholipid phases, one gramicidin-poor and one gramicidin-rich, over the range of compositions where $[Ca^{2+}]^*_f$ was virtually constant (by application of the Gibbs phase rule; see

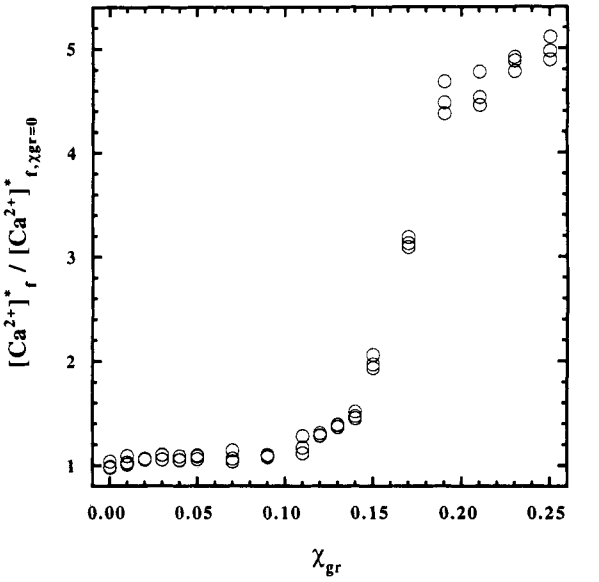

FIGURE 4: Normalized equilibrium free Ca^{2+} concentration in the bulk aqueous phase ($[Ca^{2+}]^*_f/[Ca^{2+}]^*_{f,\chi gr=0}$; denominator is 0.53 μM) as a function of χ_{gr} for gramicidin A′/DOPS dispersions at 20 °C. Each sample had 0.5 μmol of DOPS, and the Ca^{2+} chelator used was BrBAPTA. Triplicate samples were prepared by protocol I, with an initial $[Ca^{2+}]_f$ of 7.1 μM.

Discussion). The compositions of the two coexisting phases are determined by the compositions at which the invariance in $[Ca^{2+}]^*_f$ begins and ends. At intermediate values of overall χ_{gr}, two phases of the boundary compositions coexist; only the amounts of the two phases vary with composition. Based on the data of Figures 2 and 3, the composition of the gramicidin-poor phase is approximately $\chi_{gr} = 0.03$ when the phospholipid component is POPS and approximately $\chi_{gr} = 0.04$ when the phospholipid component is POPS/POPC (1/4, mol/mol). The composition of the gramicidin-rich phase is approximately $\chi_{gr} = 0.13$ when the phospholipid component is either POPS or POPS/POPC (1/4, mol/mol). The compositions at which the invariance in $[Ca^{2+}]^*_f$ begins and ends were more difficult to estimate when the phospholipid component was DOPS. Indeed, we cannot make a reasonable estimate of the composition of the gramicidin-poor phase based on the data of Figure 4. The composition of the gramicidin-rich phase was difficult to estimate with the gramicidin A′/DOPS dispersions because, although $[Ca^{2+}]^*_f$ increased very sharply with increasing χ_{gr} in the range χ_{gr} = 0.14–0.19, $[Ca^{2+}]^*_f$ also increased somewhat with increasing χ_{gr} in the range χ_{gr} = 0.09–0.14. On the basis of our ^{31}P NMR spectroscopy results (see below), we estimate that the composition of the gramicidin-rich phase is closer to $\chi_{gr} = 0.14$ than to $\chi_{gr} = 0.09$ when the phospholipid component is DOPS.

At mole fractions of gramicidin A′ greater than that of the gramicidin-rich phase, $[Ca^{2+}]^*_f$ increased with increasing χ_{gr}. The increase of $[Ca^{2+}]^*_f$ with increasing χ_{gr} became less pronounced at high values of χ_{gr} (i.e., $\chi_{gr} > 0.23$ for POPS samples, $\chi_{gr} > 0.15$ for POPS/POPC (1/4, mol/mol) samples, and $\chi_{gr} > 0.19$ for DOPS samples). Although the data at these high values of overall χ_{gr} are not precise enough for us to make a strong inference, it is possible that $[Ca^{2+}]^*_f$ again becomes independent of χ_{gr}, implying another phase separation. If such is the case, the phase richer in peptide might be lipid-poor (or lipid-free) aggregates of gramicidin A′.

Dependence of $[Ca^{2+}]^*_f$ on χ_{POPC} in POPC/POPS Multilamellar Vesicles. As a control, an equilibrium Ca^{2+}-binding experiment was performed without gramicidin A′. In this experiment, $[Ca^{2+}]^*_f$ was determined as a function of χ_{POPC}

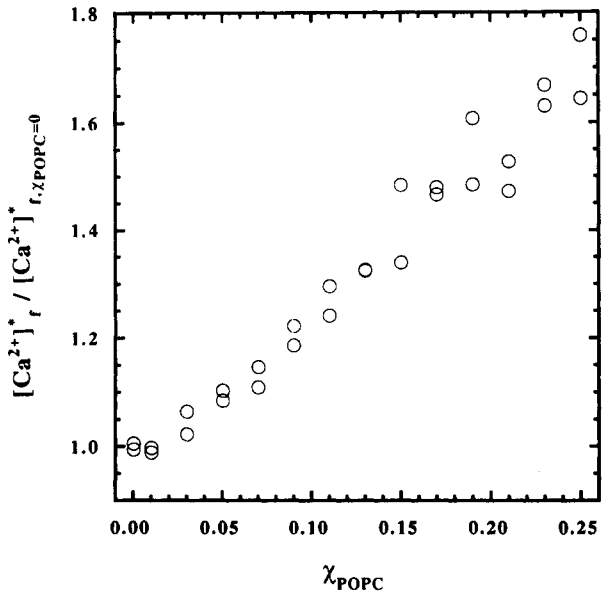

FIGURE 5: Normalized equilibrium free Ca^{2+} concentration in the bulk aqueous phase ($[Ca^{2+}]^*_f/[Ca^{2+}]^*_{f,\chi POPC=0}$; denominator is 15 nM) as a function of χ_{POPC} for POPC/POPS multilamellar vesicles at 20 °C. Each sample had 1 μmol of POPS, and the Ca^{2+} chelator used was MeBAPTA. Duplicate samples were prepared by protocol I, with an initial $[Ca^{2+}]_f$ of 0.12 μM.

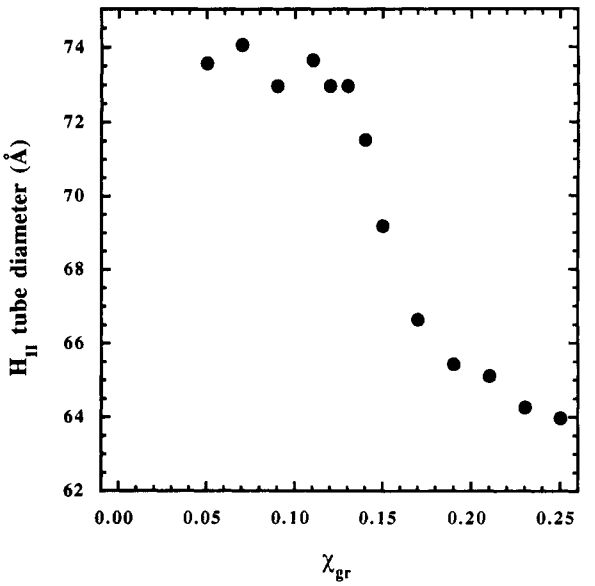

FIGURE 6: H_{II} tube diameter as a function of χ_{gr} for gramicidin A′/(POPS/POPC; 1/4, mol/mol) dispersions at ~23 °C. Each sample was hydrated (at 8 mM lipid) with 20 mM Pipes, 100 mM KCl, and 0.1 mM EDTA, pH 7.0. Each sample was exposed to 0.94-Å X-rays for 2–4 min with a sample-to-film distance of 180 mm. H_{II} tube diameter was calculated as described in the text.

Table 1: Low-Angle X-ray Diffraction Measurements of Gramicidin A′/Phospholipid Dispersions[a]

		Bragg reflections (Å) which relate as indicated to the first-order reflection						
phospholipid	χ_{gr}	1/1	$1/\sqrt{3}$	1/2	$1/\sqrt{7}$	1/3	$1/\sqrt{12}$	1/4
POPS	0	75	ND[b]	37	ND	ND	ND	19
	0.08	63.7	37.0	31.5	ND	ND	ND	ND
	0.15	62.4	37.0	32.2	24.6	21.1	18.5	ND
	0.20	58.7	33.7	30.0	22.6	19.9	17.2	ND
	0.25	58.7	33.7	28.8	22.2	ND	17.7	ND
POPS/POPC	0	75	ND	38	ND	ND	ND	19
(1/4, mol/mol)	0.08	61.1	36.1	30.6	23.3	20.3	17.7	ND
	0.15	59.9	34.8	30.0	22.9	20.4	17.4	ND
	0.20	51.6	31.2	27.0	20.7	18.0	15.3	ND
	0.25	51.6	30.9	ND	20.3	17.2	ND	ND
DOPS	0	75	ND	38	ND	ND	ND	19
	0.08	58.7	35.7	30.3	ND	20.0	17.5	ND
	0.15	57.6	33.7	29.7	ND	19.8	17.0	ND
	0.20	51.6	30.9	27.0	ND	17.9	15.5	ND
	0.25	51.6	30.3	26.3	ND	17.9	15.2	ND

[a] L_α Bragg reflections (χ_{gr} = 0) and H_{II} Bragg reflections (χ_{gr} = 0.08–0.25) at ~23 °C. Each sample was hydrated (at 3.3 mM lipid) with 5 mM Pipes, 100 mM KCl, and 0.1 mM EDTA, pH 7.0. Each sample was exposed to 1.41-Å X-rays for 5 min with a sample-to-film distance of 106 mm. [b] ND, not detected.

in POPC/POPS multilamellar vesicles. In contrast to the mixtures containing gramicidin A′, $[Ca^{2+}]^*_f$ was found to vary continuously with composition throughout the entire range of compositions analyzed (χ_{POPC} = 0–0.25; Figure 5). These data are consistent with miscibility of POPC and POPS in multilamellar vesicles from χ_{POPC} = 0 to χ_{POPC} = 0.25 (i.e., there is no phase separation).

Low-Angle X-ray Diffraction of Gramicidin A′/Phospholipid Dispersions. The gramicidin-poor and gramicidin-rich phospholipid phases were characterized by low-angle X-ray diffraction. The low-angle Bragg reflections detected at χ_{gr} = 0, 0.08, 0.15, 0.20, and 0.25 when the phospholipid component was POPS, POPS/POPC (1/4, mol/mol), or DOPS are given in Table 1. With each type of gramicidin A′/phospholipid mixture, Bragg reflections indicative of an H_{II} phase were clearly evident when χ_{gr} = 0.08–0.25. A reflection at a distance which relates as $1/\sqrt{3}$ to the H_{II} first-order reflection was observed in each case, with additional reflections at distances which relate as 1/2, $1/\sqrt{7}$ 1/3, and $1/\sqrt{12}$ to the H_{II} first-order reflection often detected as well. This series of Bragg reflections is characteristic of an H_{II} phase (Luzzati, 1980). When χ_{gr} = 0, only Bragg reflections indicative of a lamellar phase were detected with each type of gramicidin A′/phospholipid mixture. The single diffuse reflection in the wide-angle region confirmed that each of these lamellar phases is an L_α phase. Due to the net negative charge on the PS headgroups, the low-angle L_α reflections were quite diffuse and difficult to measure accurately. When χ_{gr} = 0.08, faint and diffuse L_α reflections were observed together with the much sharper H_{II} reflections with each type of gramicidin A′/phospholipid mixture (only the measurements for the H_{II} reflections are included in Table 1). No L_α reflections were observed when χ_{gr} = 0.15–0.25. Taken together, these low-angle X-ray diffraction measurements demonstrate that in each of these gramicidin A′/phospholipid systems the two phospholipid phases which coexist are a gramicidin-poor L_α phase and a gramicidin-rich H_{II} phase.

In order to estimate the compositions of the coexisting L_α and H_{II} phases in gramicidin A′/(POPS/POPC; 1/4, mol/mol) dispersions, additional low-angle X-ray diffraction measurements were made with smaller increments in χ_{gr} between each sample. Only L_α reflections were observed when χ_{gr} = 0–0.04, and only H_{II} reflections were observed when χ_{gr} = 0.11–0.25. When χ_{gr} = 0.05–0.09, both L_α and H_{II} reflections were detected together. Again, the L_α reflections were quite diffuse and difficult to measure, but at all compositions where L_α reflections were detected the L_α repeat distance was within the range 75–80 Å. At those compositions where H_{II} reflections were detected, the H_{II} tube diameter was calculated, following Luzzati (1980), as the average of $2\sqrt{3}/3$ times the first order H_{II} reflection and 2 times the reflection which relates as $1/\sqrt{3}$ to the H_{II} first order reflection (Figure 6). The H_{II} tube diameter was found to be essentially invariant from the lowest χ_{gr} where H_{II} reflections were detected (χ_{gr} = 0.05) to χ_{gr} = 0.13. However, when χ_{gr} >

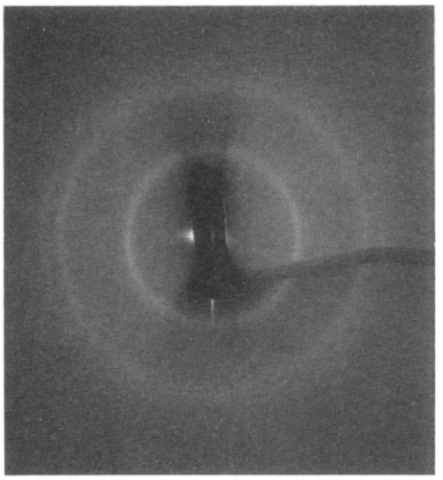

FIGURE 7: Photograph of the X-ray diffraction pattern for gramicidin A′/POPS at χ_{gr} = 0.07 at ~23 °C, indicating coexistence of H_{II} and L_α phases. Three reflections are clearly visible. The least intense of these is the reflection which relates as 1/2 to the first-order reflection and indicates L_α phase (this reflection is much less intense in pure H_{II} samples). The reflection at slightly smaller spacing relates as $1/\sqrt{3}$ to the first-order reflection and indicates H_{II} phase. The sample was hydrated (at 6 mM lipid) with 20 mM Pipes and 100 mM KCl, pH 7.0, and was exposed to 1.19-Å X-rays for 5 min with a sample-to-film disance of 430 mm.

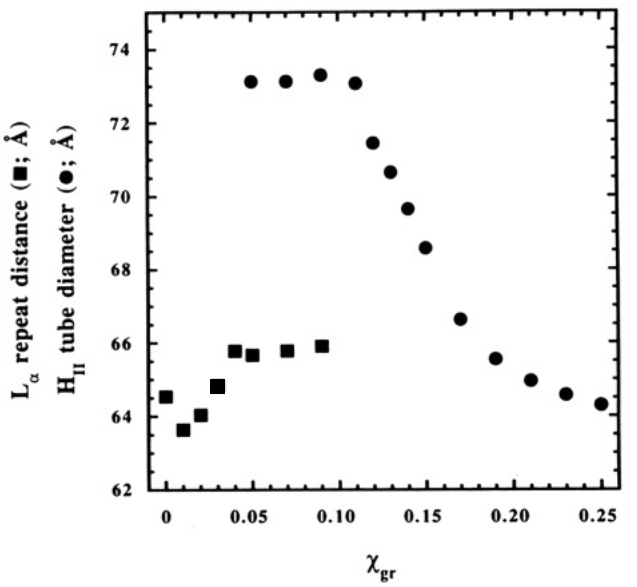

FIGURE 8: L_α repeat distance (■) and H_{II} tube diameter (●) as a function of χ_{gr} for gramicidin A′/POPC dispersions at ~23 °C. Buffer and X-ray diffraction conditions as described for Figure 7. L_α repeat distance and H_{II} tube diameter were calculated as described in the text.

0.13, the H_{II} tube diameter decreased with increasing χ_{gr}, most likely due to the dehydrating effect of gramicidin A′, or else to the intrinsic curvature of the gramicidin A′. We attribute this behavior to the coexistence of an L_α phase with χ_{gr} somewhat less than 0.05 and an H_{II} phase with $\chi_{gr} \sim 0.13$ throughout this range of compositions. These estimates of the phase boundaries are consistent with those made for this system by equilibrium Ca^{2+} binding.

In order to obtain less diffuse L_α Bragg reflections, low-angle X-ray diffraction measurements were made with gramicidin A′/POPC dispersions. For χ_{gr} between 0.05 and 0.09, both L_α and H_{II} reflections were detected together. A representative diffraction pattern is shown in Figure 7. At those compositions where L_α reflections were detected, the L_α repeat distance was calculated as the average of the L_α first-order reflection and 2 times the reflection which relates as 1/2 to the L_α first-order reflection (Luzzati, 1980), as shown in Figure 8. The L_α repeat distance was virtually constant from χ_{gr} = 0.04 to the highest χ_{gr} where L_α reflections were detected (χ_{gr} = 0.09). However, when $\chi_{gr} < 0.04$, the L_α repeat distance varied with gramicidin A′ content. The dependence of H_{II} tube diameter on χ_{gr} in gramicidin A′/POPC dispersions was very similar to the case where the phospholipid component was POPS/POPC (1/4, mol/mol). We infer from these data that, with gramicidin A′/POPC dispersions, an L_α phase with $\chi_{gr} \sim 0.04$ and an H_{II} phase with $\chi_{gr} \sim 0.11$ coexist throughout this range of compositions.

^{31}P NMR Spectroscopy of Gramicidin A′/Phospholipid Dispersions. ^{31}P NMR spectroscopy can be used to detect the coexistence of L_α and H_{II} phases (Cullis & de Kruijff, 1979). ^{31}P NMR spectra of gramicidin A′/DOPS dispersions were obtained at various compositions from χ_{gr} = 0 to χ_{gr} = 0.25. Four representative spectra are shown (Figure 9). When $\chi_{gr} < \sim 0.05$, the spectral line shape was dominated by a highfield peak and a broad lowfield shoulder characteristic of an L_α phase (e.g., Figure 9A). When $\chi_{gr} > \sim 0.12$, the spectral line shape was dominated by a lowfield peak and a highfield shoulder, with approximately half the line width relative to the L_α line shape, characteristic of an H_{II} phase (e.g., Figure 9D). When χ_{gr} = 0.091, the spectrum clearly shows both L_α and H_{II} line shapes together (Figure 9C). This spectrum also has a small, but significant, peak at 0 ppm. When χ_{gr} = 0.071, an L_α line shape is clearly evident in the spectrum but no H_{II} line shape is detectable; however, there is a large peak

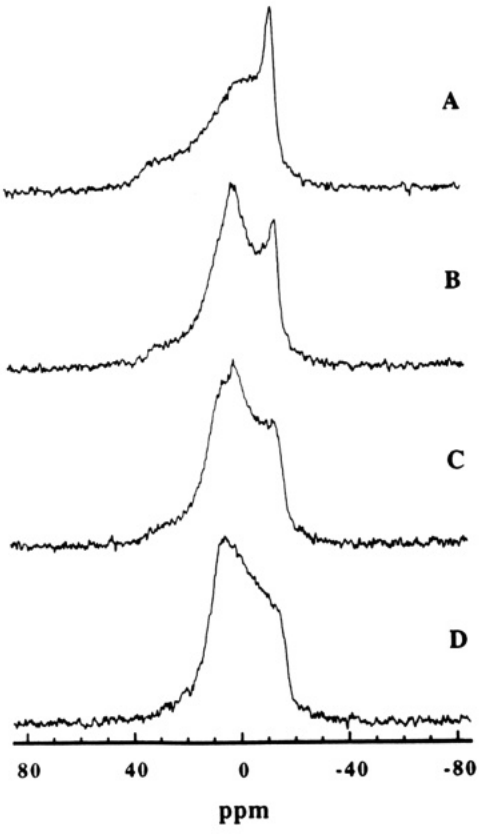

FIGURE 9: ^{31}P NMR spectra of gramicidin A′/DOPS dispersions at 20 °C and (A) χ_{gr} = 0.048, (B) χ_{gr} = 0.071, (C) χ_{gr} = 0.091, and (D) χ_{gr} = 0.125. The instrument settings were as follows: sweep width, 50 kHz; pulse width, 10 μs; acquisition time, 50 ms; receiver delay, 1 s; number of transients, 2000. An exponential multiplication corresponding to line broadening of 50 Hz was applied to the accumulated free induction decays prior to Fourier transformation. 0 ppm corresponds to the chemical shift of sonicated vesicles.

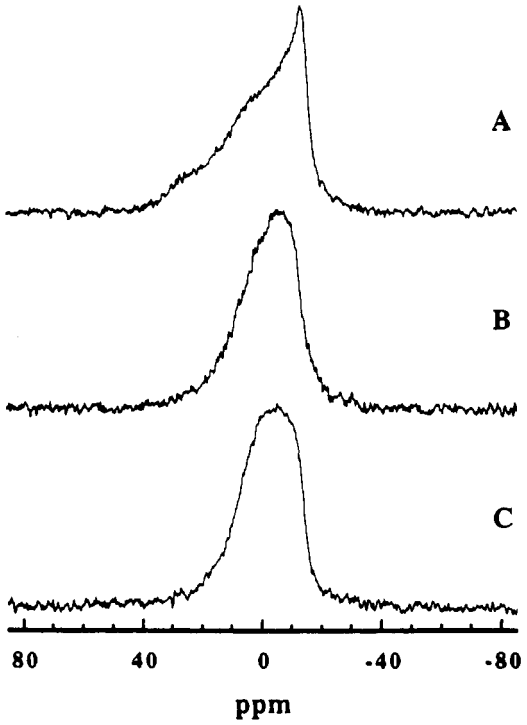

FIGURE 10: ^{31}P NMR spectra of gramicidin A′/phospholipid dispersions at 20 °C and $\chi_{gr} = 0.15$ with the phospholipid component being (A) POPS, (B) POPS/POPC (1/4, mol/mol), and (C) POPC. The instrument settings were as in the legend to Figure 8, except that the number of transients was 3000.

at 0 ppm (Figure 9B). This kind of broad symmetric peak is attributed to structures with high negative curvature, where the phospholipids can undergo isotropic motion on the NMR time scale, e.g., inverted micelles (see Discussion). Taken together, the ^{31}P NMR spectra show that a gramicidin-poor L_α phase and a gramicidin-rich inverted phase coexist throughout a wide range of compositions in the gramicidin A′/DOPS dispersions.

In sharp contrast to the ^{31}P NMR spectroscopy results obtained with gramicidin A′/DOPS dispersions, a line shape characteristic of an H_{II} phase was not observed with gramicidin A′/phospholipid dispersions when the phospholipid component was POPS, POPS/POPC (1/4, mol/mol), or POPC at any of the compositions analyzed (χ_{gr} = 0–0.25). Three representative spectra are shown (Figure 10).

DISCUSSION

By means of the Ca^{2+}-binding assay, equilibrium formation of a small amount of the $Ca(PS)_2$ phase is used to probe the fluid phase behavior of gramicidin A′/phospholipid mixtures. The bulk aqueous free Ca^{2+} concentration at equilibrium is so low (on the order of 20 nM for the gramicidin A′/POPS samples) that Ca^{2+} binding to the surfaces of the gramicidin A′/phospholipid fluid phase(s) of interest should be negligible (McLaughlin et al., 1981; Nir et al., 1978). We also point out that the samples must be multilamellar, since the $Ca(PS)_2$ phase forms by Ca^{2+} binding between lamellae. Vesicles formed by protein reconstitution methods such as detergent dialysis might not be suitable for these equilibrium Ca^{2+}-binding measurements, either because they are uni- or paucilamellar or else because an ectodomain of the protein could interfere with $Ca(PS)_2$ formation between lamellae. However, we point out that the first report of Ca^{2+}-induced phase separation leading to protein clearing described reconstituted Ca^{2+}ATPase from sarcoplasmic reticulum, a protein having a large ectodomain (London & Feigenson, 1981).

The equilibration of Ca^{2+} across lamellae is an important issue for the use of this method. Tightly sealed multilamellar vesicles give rise to elevated $[Ca^{2+}]^*_f$ values. This kind of artifact was observed with gramicidin A′/POPS dispersions when $0 < \chi_{gr} < 0.03$. The use of cellulose ester filters to support the lipid multilayers (protocol IV) has been shown to enable rapid equilibration of Ca^{2+} across lamellae (Feigenson, 1989). We found that protocol IV alleviated the elevated $[Ca^{2+}]^*_f$ artifacts when $0 < \chi_{gr} < 0.03$. At all other compositions, each of the four protocols yielded similar results, i.e., $[Ca^{2+}]^*_f$ was essentially invariant for $0.03 \leq \chi_{gr} \leq 0.13$, and $[Ca^{2+}]^*_f$ increased with increasing χ_{gr} for $\chi_{gr} > 0.13$.

Our earlier studies used the equilibrium Ca^{2+}-binding assay to determine the thermodynamic activity of PS, a_{PS}, as a function of composition in several PC/PS binary mixtures (Huang et al., 1993). In this way, the deviations from ideal, or random, mixing of PC and PS components in an L_α phase were evaluated. With mixtures of PS and a membrane-spanning peptide, measurements of $[Ca^{2+}]^*_f$ as a function of composition potentially could be used in a similar way to determine a_{PS} throughout those compositions where one gramicidin A′/phospholipid phase exists. With the gramicidin A′/phospholipid systems analyzed in this study, however, the positive deviations from ideal mixing (i.e., peptide–peptide and phospholipid–phospholipid interactions favored over peptide–phospholipid interactions) were so extreme that phase separation occurred over a wide range of compositions. The one-phase L_α region (χ_{gr} = 0 to χ_{gr} = 0.03–0.04) was not extensive enough to allow meaningful evaluations of a_{PS} as a function of χ_{gr}. Therefore, in this report we describe the usefulness of the equilibrium Ca^{2+}-binding technique in detecting the coexistence of two fluid phospholipid phases in model membranes. This study examines phase separation in gramicidin A′/phospholipid mixtures where the coexistence of L_α and H_{II} phases can be verified by independent methods. An advantage of the equilibrium Ca^{2+}-binding technique is that it is a thermodynamic approach which can be used to probe for a variety of types of phospholipid phase separations, including L_α^1/L_α^2 phase separations, which may not be easily detectable by other techniques. With the equilibrium Ca^{2+}-binding procedure, fluid phospholipid phase separation over a range of compositions is inferred directly, by application of the Gibbs phase rule, from the invariance of the measured values of the intensive variable used to calculate a_{PS}, i.e., $[Ca^{2+}]^*_f$. This is directly analogous to the familiar inference of phase separation in ordinary liquid mixtures when the intensive variable, partial pressure, is constant over a range of compositions (Lewis & Randall, 1923; French et al., 1979).

We apply the phase rule to our experimental system as follows. The gramicidin A′/phospholipid mixtures examined in this study each have four components which can be independently varied and which affect the equilibrium reaction given by eq 1. These four components are gramicidin A′, phospholipid, Ca^{2+}, and H_2O.[2] When the $Ca(PS)_2$ phase is formed from a small proportion of the PS in a sample, the

[2] Gramicidin A′ is considered one component even though it is actually a mixture of several peptides. This is permitted because the proportion of the different peptides in the gramicidin A′ mixture is constant; the mole fractions of gramicidins A, B, and C are not independently varied. Similarly, with the gramicidin A′/(POPS/POPC; 1/4, mol/mol) dispersions, the mixture of phospholipids is considered one component because the mole ratio of POPS to POPC was held constant throughout the experiment (Denbigh, 1955).

system has at least three phases: an aqueous phase, $Ca(PS)_2$, and at least one gramicidin A′/phospholipid phase. In the case of four components, three phases, and constant temperature and pressure, the variance of the system is 1. $[Ca^{2+}]^*_f$ values which vary continuously with χ_{gr} are consistent with a variance of 1 in our experimental system. Under these circumstances, the nonideality of mixing of membrane components can be analyzed as in Huang et al. (1993). However, if a fourth phase (i.e., a second gramicidin A′/phospholipid phase) appears, then the variance of the system becomes 0 throughout the entire range of compositions where a total of four phases coexist. All intensive variables are fixed throughout this range of compositions. Only the relative amounts of the coexisting phases change from one value of overall χ_{gr} to another. Thus, $[Ca^{2+}]^*_f$ values which are invariant over a range of compositions indicate a total of four coexisting phases in our experimental system of four components. We infer from the equilibrium Ca^{2+}-binding data that four phases coexist over a wide range of compositions with all three gramicidin A′/phospholipid mixtures studied. These four phases are an aqueous phase, $Ca(PS)_2$, a gramicidin-poor phospholipid phase, and a gramicidin-rich phospholipid phase.

It has been shown that a gramicidin-poor L_α phase and a gramicidin-rich H_{II} phase coexist in several gramicidin A′/phospholipid mixtures (Van Echteld et al., 1981, 1982; Killian & de Kruijff, 1985a,b; Killian et al., 1987; Watnick et al., 1990), including one of the gramicidin A′/phospholipid systems analyzed in this study: gramicidin A′/DOPS (Killian et al., 1986). Our low-angle X-ray diffraction measurements confirm that a gramicidin-poor L_α phase and a gramicidin-rich H_{II} phase coexist in gramicidin A′/DOPS dispersions and extend this result to gramicidin A′/phospholipid dispersions where the phospholipid component is POPS, POPS/POPC (1/4, mol/mol), or POPC. Low-angle X-ray diffraction was also used to estimate the phase boundaries in gramicidin A′/(POPS/POPC; 1/4, mol/mol) and gramicidin A′/POPC dispersions. The phase boundaries estimated in this way agree very well with those estimated from the equilibrium Ca^{2+}-binding data. In addition, Killian and coworkers have estimated the compositions of the coexisting L_α and H_{II} phases in gramicidin A′/DOPC dispersions by sucrose-density centrifugation (Killian et al., 1987). They found that the composition of the gramicidin-poor L_α phase is $\chi_{gr} \sim 0.06$ and the composition of the gramicidin-rich H_{II} phase is $\chi_{gr} \sim 0.13$. These phase boundaries are quite similar to those estimated in this study.

^{31}P NMR spectroscopy often yields spectra that clearly distinguish between L_α and H_{II} phases. However, we found this method to be unreliable. With the gramicidin A′/phospholipid H_{II} phases studied, only when the phospholipid component was DOPS was a ^{31}P NMR line shape characteristic of an H_{II} phase observed. When the phospholipid component was POPS, POPS/POPC (1/4, mol/mol), or POPC, the ^{31}P NMR line shape at high χ_{gr} showed some narrowing compared with that for an L_α phase, but without the characteristic lowfield peak with a highfield shoulder. There are at least three reports in the literature of gramicidin-rich H_{II} phases going undetected by ^{31}P NMR spectroscopy (Tournois et al., 1987; Gasset et al., 1988; Killian et al., 1989). The inability of ^{31}P NMR spectroscopy to detect certain gramicidin-rich H_{II} phases could arise from an altered reorientation axis of the phosphorus chemical shift tensor in these phases (Thayer & Kohler, 1981) or, more likely, from a sufficiently slow rate of phospholipid lateral diffusion around the axes of the H_{II} tubes (Burnell et al., 1980; Tournois et al., 1987). Low-angle X-ray diffraction is not influenced by these molecular motions and is therefore a more reliable technique for probing for H_{II} phases.

^{31}P NMR spectroscopy could detect both L_α and inverted phase spectral line shapes with the gramicidin A′/DOPS dispersions and so was somewhat useful in resolving the phase boundaries of this system. The ^{31}P NMR spectrum when $\chi_{gr} = 0.071$ has no spectral line shape characteristic of an H_{II} phase, but there is a large peak at 0 ppm (Figure 9B). This kind of broad symmetric peak has been ascribed to the isotropic motion of phospholipids in inverted micellar structures (Cullis & de Kruijff, 1978). Such structures between apposed bilayers may be discontinuous precursors to coalesced bundles of H_{II} tubes (Siegel, 1986). Because the ^{31}P NMR spectrum when $\chi_{gr} = 0.048$ has only a small peak at 0 ppm, and this peak is not observed when $\chi_{gr} < 0.024$, we infer that the gramicidin-poor phase boundary is somewhat less than $\chi_{gr} = 0.048$. The gramicidin-rich phase boundary was difficult to estimate from our equilibrium Ca^{2+}-binding data due to a small increase in $[Ca^{2+}]^*_f$ with increasing χ_{gr} in the range $\chi_{gr} = 0.09$–0.14 (Figure 4). Because a spectral line shape characteristic of an L_α phase is seen in the ^{31}P NMR spectrum of gramicidin A′/DOPS dispersions when $\chi_{gr} = 0.091$ (Figure 9C) and probably also when $\chi_{gr} = 0.125$ (Figure 9D), we infer that the gramicidin-rich phase boundary is closer to $\chi_{gr} = 0.14$ than to $\chi_{gr} = 0.09$.

It has been proposed that a mismatch between the length of gramicidin A′ and the length of the phospholipid acyl chains is required for H_{II} phase formation (Van Echteld et al., 1982; Killian et al., 1989). Van Echteld and co-workers (1982) showed that, at $\chi_{gr} = 0.091$, gramicidin A′ induces a significant amount of an H_{II} phase when the phospholipid acyl chains both have 18 or more carbon atoms, but not when the acyl chains both have sixteen or fewer carbon atoms. Subsequently, Watnick et al. (1990) found that gramicidin A′ can induce an H_{II} phase when the phospholipid component is DPPC (both acyl chains have 16 carbon atoms), but not until the composition of the L_α phase is $\chi_{gr} = 0.1$. Consistent with these results, we found that gramicidin A′ induced a gramicidin-rich H_{II} phase at relatively low χ_{gr} when the phospholipid was DOPS (both acyl chains have 18 carbon atoms). In addition, we found that when the phospholipid component of the mixtures had 18 carbon atoms in the *sn*-2 acyl chain but only 16 carbon atoms in the *sn*-1 acyl chain (POPS and POPC), gramicidin A′ still induced an H_{II} phase, with approximately the same phase boundaries as with DOPS.

Another kind of gramicidin A′/lipid mixture where the components exhibit positive deviations from ideal mixing large enough to lead to phase separation is gramicidin A′/lysophosphatidylcholine. Cavatorta et al. (1982) found that there are significant intermolecular tryptophan–tryptophan interactions when gramicidin A′ is incorporated into fluid lysophosphatidylcholine dispersions. Subsequent experiments showed that these dispersions can be separated into gramicidin-poor micelles (χ_{gr} was reported to vary from less than 0.01 to about 0.025) and gramicidin-rich vesicles ($\chi_{gr} \sim 0.1$), with significant tryptophan–tryptophan interactions in the latter phase (Spisni et al., 1983). These findings are analogous to the results presented here.

This study confirms that two fluid phospholipid phases can coexist in chemically simple lipid mixtures containing the membrane-spanning peptide gramicidin A′. The coexistence of multiple fluid phases in biological membranes is an intriguing possibility. Macroscopic phase separation in natural

membranes could play an important role in a wide variety of biological processes, by means of the enzymatic or physiological specialization of specific membrane regions. Macroscopic phase separation can lead to regions of the membrane having a composition very different from the overall composition. Such regions could represent recognition sites or localized protein microenvironments (Sweet & Schroeder, 1988). Changes in the size or connectivity of these regions could modulate the physical interactions and the chemical reactions of the components (Thompson et al., 1992). Determining the physiological role of macroscopic fluid–fluid phase separations in biological membranes promises to be a productive and exciting area of research.

This study introduces a novel way to detect the coexistence of two fluid phospholipid phases in model membranes. In the present work, the two coexisting phases are distinguished by ^{31}P NMR spectroscopy and/or low-angle X-ray diffraction; these physical techniques firmly establish that phase separation is indeed occurring in the systems analyzed here. An advantage of the equilibrium Ca^{2+}-binding method is that it is a thermodynamic approach which detects phase separations and defines phase boundaries by application of the Gibbs phase rule. The method does not rely on the coexisting phases having significantly different physical properties; phase separation is manifested by the invariance of an intensive variable of the system. Thus, equilibrium Ca^{2+} binding is a generally applicable method which can be used to probe for phospholipid phase separations involving phases which are physically quite similar (e.g., two L_α phases) and thus not easily discernible by other techniques. For instance, we predicted that two L_α phases coexist at equilibrium in certain PC/PS mixtures based on Monte Carlo simulations of PC/PS mixing in fluid bilayers (Huang et al., 1993). The equilibrium Ca^{2+}-binding technique has enabled us to experimentally test these predictions and to confirm that L_α^1/L_α^2 phase coexistence occurs over a range of compositions in several PC/PS mixtures (Hinderliter et al., 1994).

ACKNOWLEDGMENT

We thank Anne Hinderliter for the preparation of the standard solutions of $CaCl_2$ and BrBAPTA, Gary Labrecque for the measurement of the K_D for BrBAPTA, and Tom Irving for technical assistance during the X-ray diffraction measurements.

REFERENCES

Burnell, E. E., Cullis, P. R., & de Kruijff, B. (1980) *Biochim. Biophys. Acta 603*, 63–69.
Cavatorta, P., Spisni, A., Casali, E., Lindner, L., Masotti, L., & Urry, D. W. (1982) *Biochim. Biophys. Acta 689*, 113–120.
Cullis, P. R., & de Kruijff, B. (1978) *Biochim. Biophys. Acta 507*, 207–218.
Cullis, P. R., & de Kruijff, B. (1979) *Biochim. Biophys. Acta 559*, 399–420.
Denbigh, K. (1955) *The Principles of Chemical Equilibrium*, 1st ed., p 186, Cambridge University Press, Cambridge.
Dibble, A. R. G., Yeager, M. D., & Feigenson, G. W. (1993) *Biochim. Biophys. Acta 1153*, 155–162.
Edidin, M. (1992) *Comments Mol. Cell. Biophys. 8*, 73–82.
Feigenson, G. W. (1986) *Biochemistry 25*, 5819–5825.
Feigenson, G. W. (1989) *Biochemistry 28*, 1270–1278.
Florine, K. I., & Feigenson, G. W. (1987) *Biochemistry 26*, 1757–1768.
French, H. T., Richards, A., & Stokes, R. H. (1979) *J. Chem. Thermodyn. 11*, 671–686.
Gasset, M., Killian, J. A., Tournois, H., & de Kruijff, B. (1988) *Biochim. Biophys. Acta 939*, 79–88.
Hauser, H., & Shipley, G. G. (1984) *Biochemistry 23*, 34–41.
Hinderliter, A. K., Huang, J., & Feigenson, G. W. (1994) *Biophys. J.* (in press).
Huang, J., Swanson, J. E., Dibble, A. R. G., Hinderliter, A. K., & Feigenson, G. W. (1993) *Biophys. J. 64*, 413–425.
Killian, J. A. (1992) *Biochim. Biophys. Acta 1113*, 391–425.
Killian, J. A., & de Kruijff, B. (1985a) *Biochemistry 24*, 7881–7890.
Killian, J. A., & de Kruijff, B. (1985b) *Biochemistry 24*, 7890–7898.
Killian, J. A., van den Berg, C. W., Tournois, H., Keur, S., Slotboom, A. J., van Scharrenburg, G. J. M., & de Kruijff, B. (1986) *Biochim. Biophys. Acta 857*, 13–27.
Killian, J. A., Burger, K. N. J., & de Kruijff, B. (1987) *Biochim. Biophys. Acta 897*, 269–284.
Killian, J. A., Prasad, K. U., Hains, D., & Urry, D. W. (1988) *Biochemistry 27*, 4848–4855.
Killian, J. A., Prasad, K. U., Urry, D. W., & de Kruijff, B. (1989) *Biochim. Biophys. Acta 978*, 341–345.
Kingsley, P. B., & Feigenson, G. W. (1979) *Chem. Phys. Lipids 24*, 135–147.
Lewis, G. N., & Randall, M. (1923) *Thermodynamics and the Free Energy of Chemical Substances*, 1st ed., pp 207–212, McGraw-Hill, New York.
London, E., & Feigenson, G. W. (1981) *Biochemistry 20*, 1939–1948.
Luzzati, V. (1980) in *Biological Membranes* (Chapman, D., Ed.) pp 71–123, Academic Press, New York.
McLaughlin, S., Mulrine, N., Gresalfi, G. V., & McLaughlin, A. (1981) *J. Gen. Physiol. 77*, 445–473.
Nir, S., Newton, C., & Papahadjopoulos, D. (1978) *Biochem. Bioenerg. 5*, 116–133.
Portis, A., Newton, C., Pangborn, W., & Papahadjopoulos, D. (1979) *Biochemistry 18*, 780–790.
Seddon, J. M. (1990) *Biochim. Biophys. Acta 1031*, 1–69.
Siegel, D. P. (1986) *Biophys. J. 49*, 1155–1170.
Spisni, A., Pasquali-Ronchetti, I., Casali, E., Lindner, L., Cavatorta, P., Masotti, L., & Urry, D. W. (1983) *Biochim. Biophys. Acta 732*, 58–68.
Sweet, W. D., & Schroeder, F. (1988) in *Advances in Membrane Fluidity* (Aloia, R. C., Curtain, C. C., & Gordon, L. M., Eds.) Vol. 2, pp 17–42, Alan R. Liss, Inc., New York.
Thayer, A. M., & Kohler, S. J. (1981) *Biochemistry 20*, 6831–6834.
Thompson, T. E., Sankaram, M. B., & Biltonen, R. L. (1992) *Comments Mol. Cell. Biophys. 8*, 1–15.
Tocanne, J. F. (1992) *Comments Mol. Cell. Biophys. 8*, 53–72.
Tournois, H., Leunissen-Bijvelt, J., Haest, C. W. M., de Gier, J., & de Kruijff, B. (1987) *Biochemistry 26*, 6613–6621.
Tsien, R. Y. (1980) *Biochemistry 19*, 2396–2404.
Urry, D. W. (1971) *Proc. Natl. Acad. Sci. U.S.A. 68*, 672–676.
Urry, D. W., Goodall, M. C., Glickson, J. D., & Mayers, D. F. (1971) *Proc. Natl. Acad Sci. U.S.A. 68*, 1907–1911.
Van Echteld, C. J. A., Van Stigt, R., de Kruijff, B., Leunissen-Bijvelt, J., Verkleij, A. J., & de Gier, J. (1981) *Biochim. Biophys. Acta 648*, 287–291.
Van Echteld, C. J. A., de Kruijff, B., Verkleij, A. J., Leunissen-Bijvelt, J., & de Gier, J. (1982) *Biochim. Biophys. Acta 692*, 126–138.
Verkleij, A. J. (1984) *Biochim. Biophys. Acta 779*, 43–63.
Watnick, P. I., Chan, S. I., & Dea, P. (1990) *Biochemistry 29*, 6215–6221.
Wolf, D. E. (1992) *Comments Mol. Cell. Biophys. 8*, 83–95.